Rheological and mechanical behavior of polyacrylamide hydrogels chemically crosslinked with allyl agarose for two-dimensional gel electrophoresis

R. Suriano[a,*], *G. Griffini*[a], *M. Chiari*[b], *M. Levi*[a], *S. Turri*[a]

[a]*Department of Chemistry, Materials and Chemical Engineering "Giulio Natta", Politecnico di Milano, Piazza Leonardo da Vinci 32, 20133 Milan, Italy*

[b]*Istituto di Chimica del Riconoscimento Molecolare, C.N.R., Via Mario Bianco 9, 20131 Milan, Italy*

Received 20 September 2013 Received in revised form
2 December 2013
Accepted 4 December 2013 Available online 11 December 2013

[*]*Corresponding author*. Tel.: +39 0223993249; fax: +39 0270638173.
E-mail address: raffaella.suriano@polimi.it (R. Suriano).

1. Introduction

In the field of proteomics, the ability to detect a large number of proteins in a single analysis represents a key issue to achieve fast and efficient operation (Rabilloud et al., 2009; Miller et al., 2010). In this context, the combined use of 2-D gel electrophoresis coupled with mass spectrometry has allowed enormous advances during last few decades and has become nowadays one of the standard approaches for protein separation and identification (Rabilloud, 2002; Görg et al., 2004; Rabilloud et al., 2010; Rogowska-Wrzesinska et al., 2013).

Among the materials used for 2-D gel electrophoresis, polyacrylamide crosslinked hydrogels have been extensively investigated in the literature because their tunable mesh size porosity appears to be ideal for separating proteins and DNA samples (Calvet et al., 2004; Manns, 2005). Typically, acrylamide concentrations higher than 5% are used to form the separation matrix, with the acrylamide concentration being selected to maximize resolution of the range of proteins of interest (Gerstner et al., 2000). Lower acrylamide concentrations are necessary when resolution of large high molecular mass (HMM) proteins (>500 kDa) is sought, however at the expense of poor mechanical stability of the gel matrix that often yields difficulties in handling these media (Suh et al., 2005). Other polymeric systems alternative to polyacrylamide gels have also been proposed as separation matrices for 2-D electrophoresis, including agarose (Oh-Ishi and Maeda, 2007; Greaser and Warren, 2012), CNTs-modified polyacrylamide gels (Parthasarathy et al., 2011) and acrylamide–agarose copolymers (Roncada et al., 2005). In particular, the advantages of the acrylamide–agarose system mainly lay in the possibility of improving the resolution of large HMM proteins without compromising the resolution of low molecular mass proteins, partly due to the optimal average pore size of these materials.

Indeed, the electrophoretic migration process through the polymeric gel matrix is driven by the interactions between the protein fragments and the porous network of the gel, causing the quality of protein resolution to be highly dependent on different structural parameters characteristic of the gel matrix (Wang and Ugaz, 2006). Among these, mean gel pore size, pore size distribution and stiffness of the gel play a crucial role. In order to achieve improved separation performance in 2-D electrophoresis applications, it is therefore essential to understand the specific nature of the pore structure of the gel and the parameters through which this pore structure can be controlled and manipulated (Anseth et al., 1996; Dumitriu et al., 2011). In particular, it is of great interest to investigate structure–property relationships of these hydrogels in the attempt to optimize their functional performance.

In this work, the rheological and mechanical properties of a series of promising acrylamide-based hydrogels chemically crosslinked with allyl agarose were studied at increasing crosslinker concentrations. As previously demonstrated (Roncada et al., 2005), this class of hydrogels was found to improve protein separation in 2-D gel electrophoresis. However, no systematic investigation on the effects of chemical composition and crosslinking density on the rheological, structural and functional properties of these systems was presented. In order to obtain optimal separation performance, a thorough understanding of the relationships between chemical composition, physical structure, mechanical and functional properties of these materials is however necessary and still to be accomplished.

In the present study, the effects of chemical composition and crosslinking density on the rheological and mechanical properties of acrylamide–allyl agarose crosslinked hydrogels were thoroughly investigated. As opposed to previous work (Roncada et al., 2005), a wide range of hydrogel chemical compositions was studied and their effect on structural and functional properties of the hydrogel was elucidated. By employing dynamic rheological tests and creep-recovery tests, a correlation was found between the rheological response of these hydrogels and their sieving properties. More specifically, the evaluation of the crosslinking density by means of dynamic tests and the use of viscoelastic models for determining the resistance of non-permanent crosslinks to move in the network systems shed light on the pore structure of the hydrogel matrix and helped to clarify its influence on the electrophoretic separation performance. In addition, the mechanical stability of the crosslinked hydrogels was investigated by means of tensile tests and correlated with the crosslinking density of the gel matrix.

The aim of this study is to achieve a greater understanding of structure–property relationships in crosslinked acrylamide–agarose hydrogels and to provide useful guidelines for the design of mechanically stable hydrogels with improved protein resolution to be employed in 2-D gel electrophoresis.

2. Experimental part

2.1. *Materials and gel preparation*

Allyl agarose was prepared as described elsewhere (Chiari et al., 1995; Chiari et al., 1996; Roncada et al., 2005). Briefly, 33 mg of sodium borohydride and 1.6 mL of allylglycidyl ether were added to a suspension of 1 g of agarose in NaOH (33 mL, 0.3 M) under stirring. After slow stirring for 12 h, allyl derivative of agarose was recovered from the suspension by filtration and then washed with distilled water up to a neutral pH. Allyl agarose was finally dehydrated in methanol and dried under vacuum at 35 °C.

Acrylamide gels crosslinked with allyl agarose were prepared by dissolving different amounts of allyl agarose (from 0.2% to 1% w/v) at 95 °C, in 0.375 M Tris–HCl buffer at pH=8.8. The solution was cooled down to 40 °C and then acrylamide (10% w/v) and sodium dodecyl sulfate, SDS (0.1% w/v) were added maintaining the solution in a thermostatic bath at 40 °C. Ammonium persulfate (APS) (0.04%) and tetramethylethylenediamine (TEMED) (0.05% v/v) were also added immediately before the solution was moved to the casting mold. Polyacrylamide standard gel (PAB) was cast using a standard procedure with 10% w/v of acrylamide and 2.6% w/v of N,N′-methylenebisacrylamide. Acrylamide, N,N′-methylenebisacrylamide, APS and TEMED were purchased from Sigma-Aldrich. Allylglycidyl ether and SDS were purchased from Fluka (Buchs, Switzerland). Agarose (low EOF) was from Amersham Biosciences (Piscataway, NJ, USA).

2.2. Rheological and mechanical characterization

Creep-recovery and oscillatory dynamic tests were carried out using a Rheometrics DSR 200 stress-controlled rheometer. The diameter of parallel-plates geometry mounted on the rheometer was 25 mm, the gap between plates 1.3 mm and the measurement temperature about 25 °C.

During creep-recovery tests, a constant value of stress (τ=700 Pa) was applied for 180 s and the shear strain γ(t) was measured (loading phase). After 180 s, the imposed stress was suddenly removed and γ(t) was measured as a function of time for further 180 s (recovery phase). Fitting of the creep curves was carried out by means of OriginPro 8 software and the quality of the fitting was evaluated in terms of coefficient of determination R^2 (the maximum number of iterations was set to 400 for each fitting).

Dynamic frequency sweep tests were performed over the frequency range of 0.1–10 Hz in the auto-stress adjustment mode, which allowed the automatic modification of the applied stress if deformation exceeded the limiting value of 7%. For dynamic stress sweep tests, two different constant values of frequency (1 and 0.1 Hz) were selected and the stress was varied from 100 to 6000 Pa. For the uncrosslinked polyacrylamide (PA), dynamic frequency sweep tests were performed using a cone-and-plate geometry with a diameter of 40 mm and a gap of 0.05 mm. Measurements were recorded in a constant stress mode (4 Pa) for frequencies ranging from 0.1 to 10 Hz at about 20 °C.

A Minimat MKII dynamometer was used to acquire stress–strain curves on 20 mm long, 4.25 mm wide and 1.7 mm thick specimens. Tensile tests were performed with a load cell of 10 N, at a rate of 100 mm/min. The measurements are presented as averages of five replicates for each type of hydrogels.

3. Results and discussion

3.1. Creep-recovery tests

The viscoelastic properties of a series of polyacrylamide hydrogels crosslinked with allyl agarose were investigated using creep-recovery experiments. Fig. 1 shows creep-recovery curves for hydrogels containing a fixed concentration of acrylamide, 10% w/v, and different amounts of allyl agarose, ranging from 0.2% to 1% w/v (for brevity, from here on these hydrogels will be referred to as PAA followed by a number indicating the concentration of allyl agarose multiplied by 10). As a comparison, the creep-recovery curve for standard polyacrylamide gel (PAB) with a concentration of acrylamide monomer T=10% w/v and a concentration of bisacrylamide as crosslinker C=2.6% w/v is also shown.

The majority of crosslinked hydrogels show the typical deformation behavior of viscoelastic solids (Fig. 1). As a result of the constant stress applied, a strain γ arises that increases steadily, showing a curved time-dependent trend; when the stress is removed, a delayed recovery takes place almost completely. The creep-recovery curves of PAA2 and, partially, PAA6 appear to be slightly different from those of the other hydrogels. Both of them recovered only part of the strain and

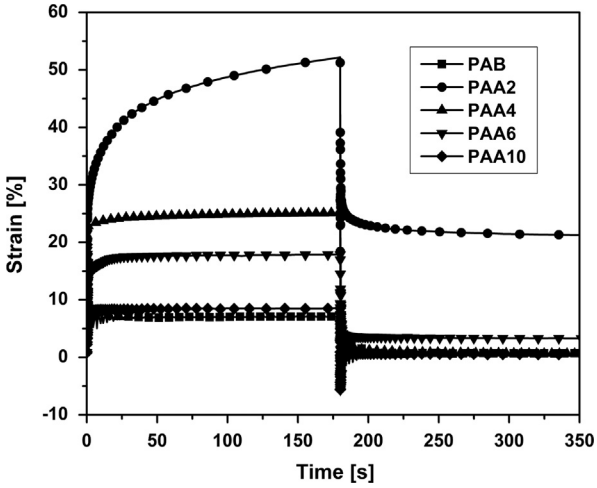

Fig. 1 – Creep-recovery curves of the materials investigated in this work.

PAA2 exhibited a permanent strain value higher than PAA6 in the recovery phase. This suggests the presence of predominant viscous deformation especially for PAA2, thus showing a partly viscoelastic fluid-like behavior. In addition, in the loading phase γ reached a plateau value after a sufficiently long period of time for all hydrogels investigated except for PAA2. The different behavior of PAA2 can be attributed to slippage of entanglements on branched structures which are incompletely attached to the macromolecular network, as a consequence of lower degree of crosslinking (Ferry, 1970). Accordingly, the presence of rearrangements of chain segments separated by entanglements in PAA2 may cause permanent deformation to remain after the loading phase. In contrast, at higher degree of crosslinking (than that of PAA2) such branched structures are present in smaller quantity and the gels exhibit equilibrium plateau compliance.

In order to analyze quantitatively the creep curves during the loading step, the Kelvin–Voigt mechanical model can be employed (Alfrey and Gurnee, 1956), consisting of a spring (elastic component) and a dashpot (viscous component) combined and arranged in parallel (Scheme 1a). According to this model, an estimate of the resulting strain γ(t) in the creep test is given by the following equation:

$$\gamma(t) = \left(\frac{\overline{\sigma}}{G}\right)\left(1-\exp\left(-\frac{t}{\lambda}\right)\right) \quad (1)$$

where $\overline{\sigma}$ is the constant shear stress applied, G is the shear modulus (corresponding to the spring constant), $\lambda=\eta/G$ is defined as the retardation time, which is a measurement of the time required for the spring to extend to its equilibrium length while retarded by the dashpot, and η is the viscosity (corresponding to the dashpot constant).

The viscoelastic function known as creep compliance J(t), which is the reciprocal value of the shear modulus G (considered as "rigidity" of the material), can be calculated as the ratio of γ(t) to $\overline{\sigma}$:

$$\frac{\gamma(t)}{\overline{\sigma}} = J(t) = J_e\left(1-\exp\left(-\frac{t}{\lambda}\right)\right) \quad (2)$$

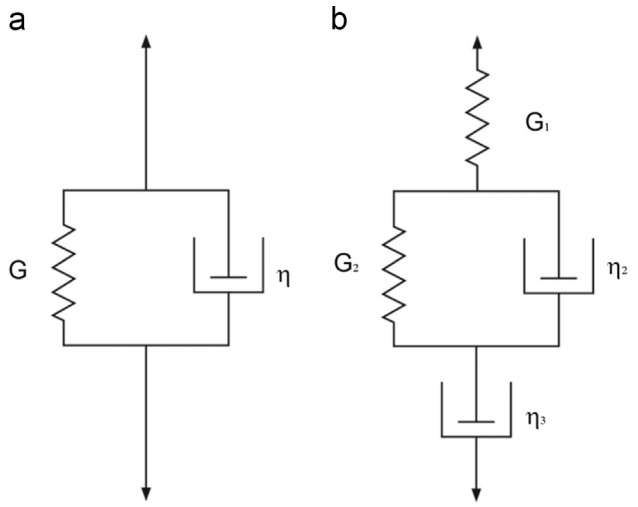

Scheme 1 – Symbolic representation of (a) Kelvin–Voigt and (b) four-parameter Voigt models.

where J_e is the equilibrium compliance, i.e. the limiting value of the $J(t)$ reached when the strain approaches its maximum value after a sufficiently long period of time.

Creep-recovery behavior of viscoelastic materials can be also predicted by a four-parameter Voigt model (Alfrey and Gurnee, 1956), also known as Burgers model, obtained by combination of three different elements in series: a spring with shear modulus G_1, a Kelvin–Voigt element (a spring with shear modulus G_2 and a dashpot with viscosity η_2 arranged in parallel) and a dashpot with viscosity η_3 (Scheme 1b). Applying this latter model, the creep compliance $J(t)$ can be expressed by the following equation:

$$J(t) = \frac{1}{G_1} + \frac{1}{G_2}\left(1 - \exp\left(-\frac{t}{\lambda_2}\right)\right) + \frac{t}{\eta_3} \quad (3)$$

where $G_1 = 1/J_1$, visible in the creep curve as a time-independent purely elastic jump and λ_2 is the retardation time of the Kelvin–Voigt element. According to Eq. (3), the compliance $J(t)$ is the sum of (a) an instantaneous elastic response, $J_1 = 1/G_1$, (b) a viscoelastic (delayed elastic) component, $J_2 = 1/G_2(1 - \exp(-t/\lambda_2))$, and (c) unrecovered viscous flow, $J_3 = t/\eta_3$.

Interpolation of creep curves of $J(t)$ allowed the determination of the parameters for Kelvin–Voigt (Eq. (2)) and Burgers (Eq. (3)) models for all hydrogels (Tables 1 and 2, respectively).

As for PAA10, the Kelvin–Voigt model gives a value of spring constant G comparable to that estimated for standard PAB. By progressively decreasing the concentration of crosslinker in the PAA gels, a gradually lower value of G is calculated by the Kelvin–Voigt model. This suggests that the network structure of the hydrogels crosslinked with lower percentage of allyl agarose has higher equilibrium compliance, J_e. Concurrently, by increasing the concentration of allyl agarose a sharp decrease of viscosity η is observed up to PAA4 and then η increases significantly for higher concentration of allyl agarose (0.6% and 1%). From examination of the data presented in Table 1 it is clear that the fitting of the PAA2 and PAA6 behavior with the two-parameter model is quite poor (low value of R^2), as a consequence of the permanent deformation shown by these materials.

Table 1 – Best fitting parameters estimated for the creep curves and obtained for each hydrogel according to the mathematical model described in Eq. (2). The standard errors for the estimated parameters were found to be less than 5% of the value of the corresponding parameter.

	G (Pa)	η (Pa s)	λ (s)	R^2
PAB	99.99	538.13	5.38	0.96
PAA2	17.12	20.62	1.20	0.53
PAA4	28.36	10.45	0.37	0.94
PAA6	41.58	29.41	0.71	0.78
PAA10	84.74	48.56	0.57	0.95

By interpolating the creep curves according to the Burgers model (Eq. (3)), higher values of R^2 were obtained for PAA2-6, as compared to those found by employing the Kelvin–Voigt model. This indicates a higher quality of parameter prediction and a higher degree of confidence in the four-parameter model, especially for PAA2-6 gels. These hydrogels also show a lower elastic component G_1 than PAB and PAA10 gels that yields a higher purely elastic compliance J_1. As will be explained in the next section ("*Sinusoidal dynamic tests*"), these values of G_1 may be explained by considering that PAA2-6 exhibit a lower crosslinking density compared to the other gels, thus leading to lower shear modulus, G_1. Concerning the viscoelastic components, the values of G_2 and η_2 for PAB and PAA10 are comparable to those calculated by the Kelvin–Voigt model. Finally, the retardation time λ_2 for PAA2-6 appears to be higher than that found in PAB and PAA systems. This parameter suggests that for PAA2-6 the influence of η_2 with respect to G_2 is greater. Since the value of η_2 is correlated with the internal frictions between macromolecular chains, this result may be associated with a higher resistance of the polymer chains to slip and stretch in order to respond to the applied stress. In addition to giving further insights into rheological behavior of the hydrogels considered, this parametric study on mechanical models also provides a clearer understanding of the results presented in a previous work about the separation of a broad range of proteins with different molecular weights by SDS-electrophoresis using PAA2-6 gels (Roncada et al., 2005). As already shown previously, both large and small proteins could be better resolved in PAA2-6 hydrogels compared to standard PAB. While the improved resolution of high molecular weight proteins provided by PAA2-6 in comparison with PAB can be explained by higher average pore size (see next section "*Sinusoidal dynamic tests*"), the formation of larger pores does not justify good resolution observed also for lower molecular weight proteins. The higher purely elastic compliances and retardation times calculated for PAA2-6 hydrogels can shed light on their good sieving properties observed for both small and large proteins (from 40 to 200 kDa). Indeed, high values of J_1 and λ_2 can be related to the fact that non-permanent crosslinks between polymer chains, e.g. strong interchain interactions and not trapped entanglements, are strong enough to delay the run of large proteins, blocking them provisionally and allowing smaller proteins to flow. Although the presence of such non-permanent crosslinks can temporarily stop the movement of high molecular weight proteins,

Table 2 – Best fitting parameters estimated for the creep curves and obtained for each hydrogel according to the mathematical model described in Eq. (3). The standard errors for the estimated parameters were found to be less than 5% of the value of the corresponding parameter.

	G_1 (Pa)	G_2 (Pa)	η_2 (Pa s)	λ_2 (s)	η_3 (Pa s)	R^2
PAB	308.33	150.74	1092.19	7.25	723,565	0.96
PAA2	26.87	44.83	523.55	11.68	10,797	0.99
PAA4	30.74	417.96	6435.46	15.40	175,537	0.99
PAA6	50.53	187.72	1597.56	8.51	439,278	0.99
PAA10	552.63	101.01	75.31	0.75	295,625	0.96

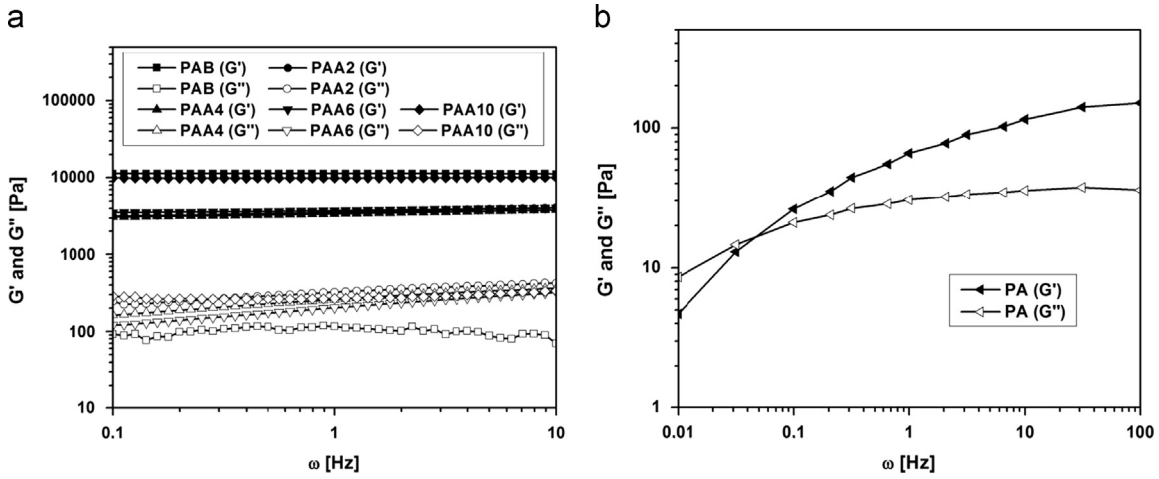

Fig. 2 – Elastic (G') and viscous (G'') components of the complex modulus for (a) PAB, PAA2, PAA4, PAA6, PAA10 and (b) for reference uncrosslinked polyacrylamide gel PA, obtained by means of dynamic frequency-sweep rheological measurements.

it does not completely prevent their run, as these non-permanent crosslinks are continuously broken and reformed during successive electrophoretic runs, eventually allowing large proteins to be resolved. This would explain why PAA2-6 hydrogels enhance the migration of large proteins giving concurrently a good resolution of smaller ones, as opposed to PAA10 and PAB.

3.2. *Sinusoidal dynamic tests*

The effect of crosslinker concentration on mechanical properties was also investigated by dynamic mechanical measurements, where the specimen is subjected to a sinusoidally oscillating stress. The storage modulus $G'(\omega)$ and loss modulus $G''(\omega)$ obtained from dynamic frequency sweep tests for PAA and PAB hydrogels are shown in Fig. 2a. As a comparison, dynamic oscillatory tests as a function of frequency were also carried out on uncrosslinked polyacrylamide gels (PA) (Fig. 2b).

Fig. 2a shows that for all crosslinked samples $G'(\omega)$ is higher than $G''(\omega)$ over the entire frequency range (0.1–10 Hz). This finding indicates that the elastic response of these hydrogels is stronger than the viscous one, indicating their predominantly solid-like behavior. In contrast, the loss modulus of uncrosslinked PA gels is higher than the storage modulus at low frequencies up to a critical frequency ω_c, defined as crossover frequency, when $G''(\omega)/G'(\omega)=1$. For these gels, the so-called sol–gel transition (from the viscous to the predominant elastic behavior) occurs at a crossover frequency of 0.04–0.05 Hz (Fig. 2b). For ordinary crosslinked PAB and PAA10 gels, $G'(\omega)$ has a constant value of approximately 11,300 Pa and 9900 Pa respectively, whereas PAA2-6 show a value of G' in the range of 3100–4100 Pa.

The mechanical stability of hydrogels was also investigated by analyzing the dependence of G' and G'' on the shear stress, τ. Fig. 3 presents the curves of G' and G'' as a function of oscillatory shear stress τ at a frequency of 1 Hz (Fig. 3a) and 0.1 Hz (Fig. 3b).

For all samples investigated, at low shear stress (<1000 Pa) the curves of G' and G'' show the presence of a linear viscoelastic zone, i.e. the range where the storage modulus is independent of the applied stress. No significant change of internal three-dimensional structure of the polymer gels occurs over this range of applied stresses until the yield stress is reached, the latter being the τ value at which the curve begins to diverge appreciably from the plateau value. The yield stress also represents the limiting value of the linear viscoelastic range and defines the onset of irreversible plastic deformation. Standard crosslinked PAB and PAA10 gels show an evident value of the yield point in stress sweep tests performed both at 0.1 and 1 Hz. On the other hand, PAA gels with lower concentration of crosslinker (0.2–0.6%) show the presence of a plateau value of G' measured at 1 Hz that extends up to higher stress values compared to PAB and PAA10. In particular, for PAA2-6, the yield point becomes noticeable only when the stress sweep test is performed at low frequency

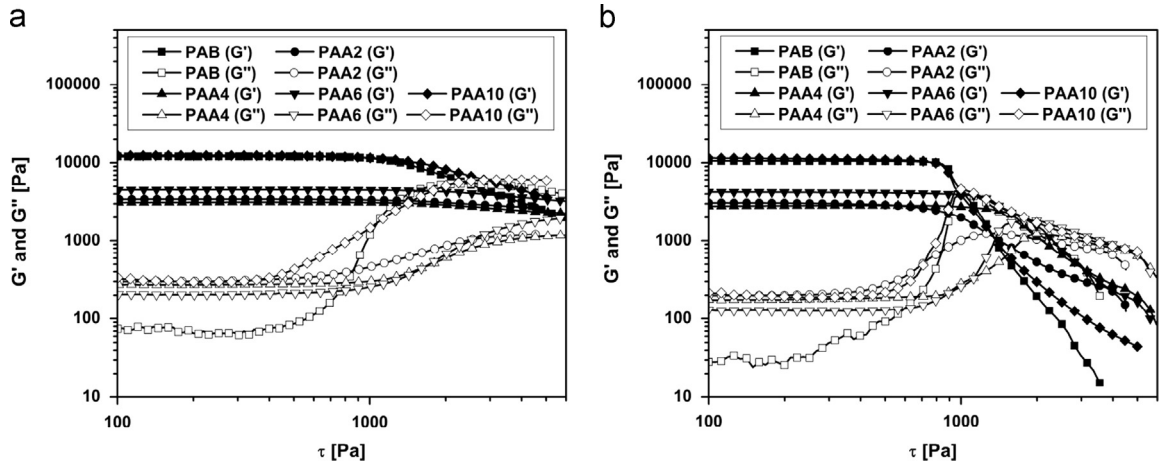

Fig. 3 – Elastic (G') and viscous (G'') components of the complex modulus for the materials investigated in this work, obtained by means of dynamic stress–sweep rheological measurements at oscillatory frequencies of (a) 1 Hz and (b) 0.1 Hz.

(0.1 Hz). In fact, in stress sweep tests performed at 1 and 0.1 Hz on PAB and PAA10 gels, G' undergoes a strong decrease for $\tau \geq 1500$ Pa and for $\tau \geq 950$ Pa, respectively. On the other hand, PAA2-6 exhibit a remarkable decrease in G' only in the test carried out at 0.1 Hz, where the yield point stress is about 1200 Pa. This difference can be attributed to a higher mechanical strength of the structure of PAA2-6, compared with PAB and PAA10. This trend is further confirmed by considering the stress value at which $G' = G''$ (critical oscillatory stress, τ_c) for all hydrogels. Indeed, for stress sweep tests performed on PAB and PAA10 gels at 0.1 Hz, τ_c (around 1000 Pa) is lower than that measured for PAA2-6 (1200–1800 Pa).

Dynamic rheological tests also allowed the calculation of the crosslinking density, namely the number of elastically active junctions in the network per unit of volume, n_e (in mol/m^3). According to the classical theory of rubber elasticity, the equilibrium shear elastic modulus of a crosslinked gel G_e is related to n_e as follows (Ferry, 1970; Calvet et al., 2004):

$$G_e = n_e RT \quad (4)$$

where R is the universal gas constant (8.314 J/(mol K)) and T is the measurement temperature (298 K). The equilibrium shear elastic modulus G_e corresponds to the plateau value of G' measured by frequency and stress sweep tests (Figs. 2 and 3, respectively).

The values of n_e were calculated based on Eq. (4) for the three different dynamic tests and are presented in Fig. 4 for all hydrogels considered in this work. As inferred from Fig. 4, a lower density of active junctions was obtained for PAA2-6, meaning that a lower number of chemical crosslinks and trapped entanglements provide a network with a wider mesh. This network structure results in a larger average pore size that explains the efficient resolution for higher molecular mass proteins observed in PAA2-6 (Roncada et al., 2005).

3.3. *Tensile tests*

Tensile tests were also performed on all hydrogels in order to observe the influence of crosslinker on mechanical behavior of hydrogels at large deformations. The shape of stress–strain

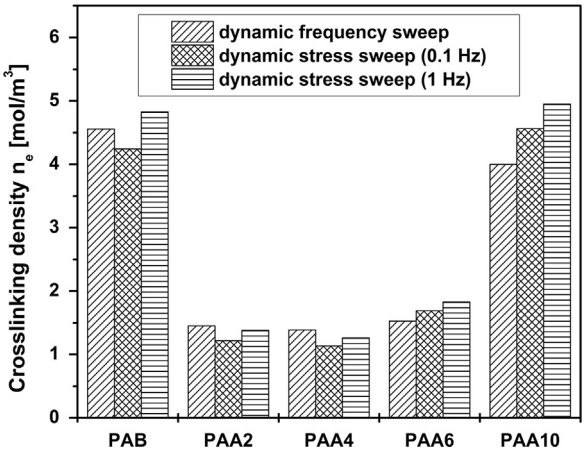

Fig. 4 – Crosslinking density n_e of the materials investigated in this work obtained from different dynamic rheological measurements, namely frequency sweep and stress sweep (0.1 Hz and 1 Hz).

curves obtained for PAA2-6 appears to be more rubber-like than for PAB and PAA10 (Fig. 5). In fact, for a given σ, significantly larger deformations are observed for PAA2-6, compared with PAA10 and PAB.

The values of stress and strain at break point (σ_r and ε_r respectively) and toughness (E_r) defined as the area underneath the entire stress–strain curve up to rupture are shown in Fig. 6. For PAB gels, the average values of σ_r and ε_r are noticeably lower than those of PAA gels (Fig. 6(a) and (b)). Gels crosslinked with 0.2% and 0.4% of allyl agarose exhibit a higher value of ε_r than other gels. However, PAA2 have a low value of σ_r, suggesting a poor mechanical strength of the hydrogel. Actually σ_r increases remarkably for the hydrogel with 0.4% of allyl agarose, leading to a higher value of toughness. Such hydrogel (PAA4) appears therefore very resistant and tough, making it the most suitable to be employed as gel for 2-D gel electrophoresis. Indeed, by further increasing the concentration of allyl agarose (PAA6 and

PAA10), a sharp decrease in ε_r is observed together with a significant reduction in toughness (Fig. 6(b) and (c)), even though the values of σ_r are comparable to that measured for PAA4. This suggests that for higher crosslinker concentrations (0.6% and 1%) the hydrogels become more brittle than PAA2 and PAA4.

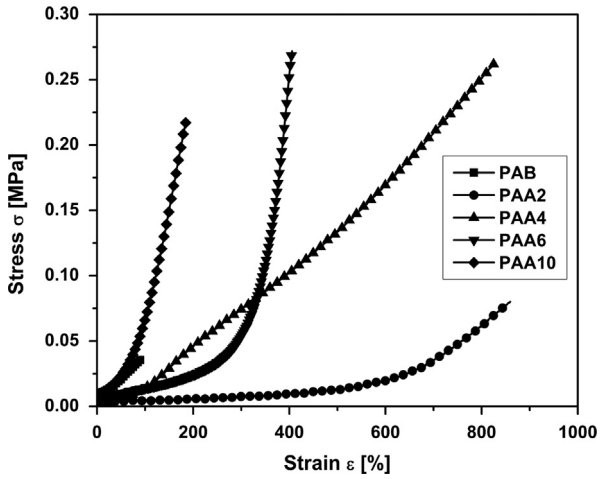

Fig. 5 – Stress–strain curves for the materials investigated in this work.

4. Conclusions

The rheological and mechanical properties of a series of hydrogels covalently crosslinked with allyl agarose (PAA) were studied by varying the concentration of crosslinking agent and were compared to chemically crosslinked polyacrylamide (PAB), typically used as a standard matrix for 2-D gel electrophoresis. Dynamic rheological tests evidence the mainly solid-like behavior of the investigated hydrogels as well as the effect of crosslinker concentration on mechanical strength. The structure of PAA with a percentage of allyl agarose between 0.2% and 0.6% shows a higher strength in comparison with standard PAB and PAA10 gels. Dynamic tests also highlight that the density of crosslinking for PAA2-6 hydrogels is lower than for the other gels and this feature provides an explanation for the remarkable improvement of electrophoretic separation of high molecular mass proteins, when PAA2-6 systems are employed.

The rheological analysis using creep-recovery tests suggests the presence of purely viscous deformation for loosely crosslinked PAA2 gel (low crosslinking density). This irreversible deformation reveals the mobility of a network featured by branched structures which undergo permanent rearrangements and changes under a constant stress. Interpolation of the creep curves according to the Kelvin–Voigt and four-parameter Voigt

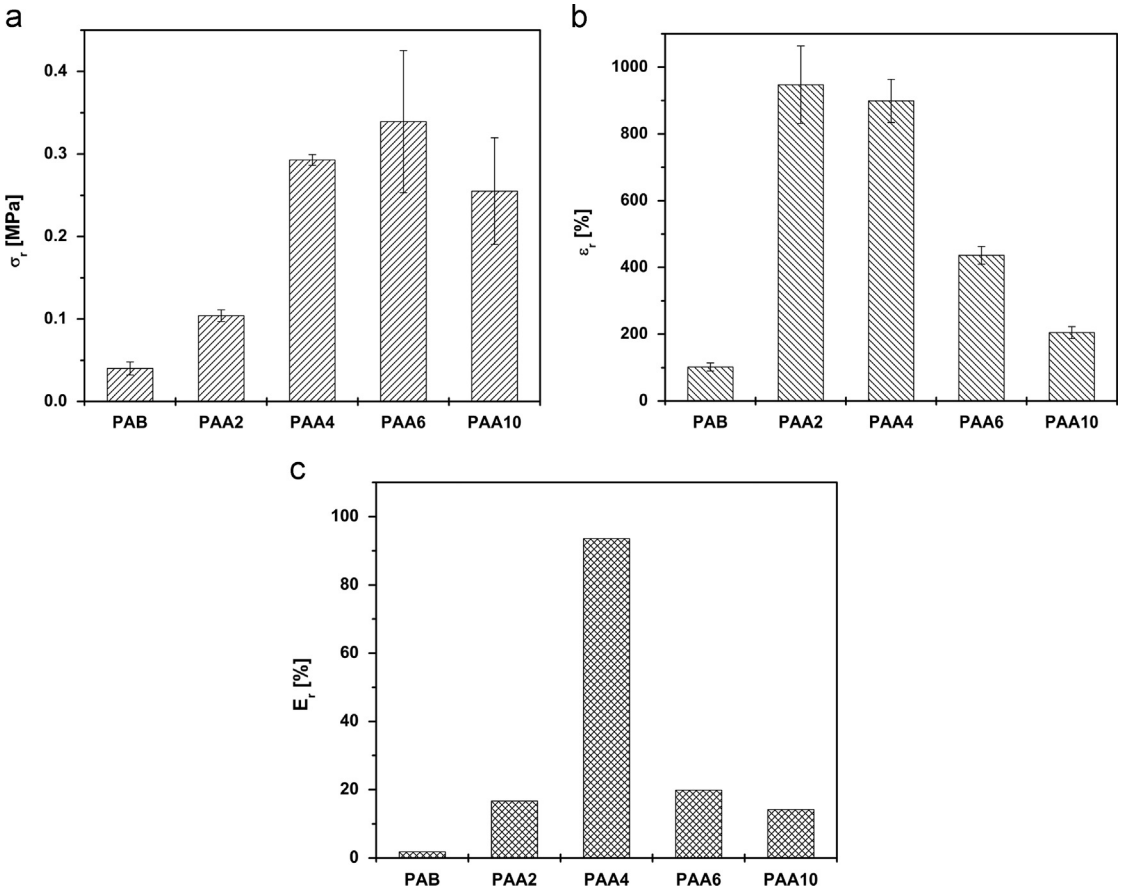

Fig. 6 – Mean values of (a) stress σ_r, (b) elongation ε_r at break point, and (c) toughness E_r for the materials investigated in this work; vertical bars represent the standard deviation.

models, provides a relationship between the mechanical properties of these hydrogels and their ability to separate small proteins during electrophoretic runs. In particular, the motion of polymer chains (e.g. the breakage/formation of strong interchain interactions or the movement of entanglements) can affect positively the sieving properties of these hydrogels with regard to low molecular mass proteins.

An optimal concentration of allyl agarose of 0.4% allows the improvement of the mechanical stability and properties of the sieving gel, while maintaining good functional performance in bidimensional electrophoresis.

In conclusion, the rheological and mechanical characterization illustrated in this study allows a better understanding of the relationships between the rheological behavior and the functional properties of these polyacrylamide-based systems and provides useful guidelines to design and fabricate hydrogels with improved resolution for both small and large proteins in 2-D gel electrophoresis.

Acknowledgments

The authors wish to thank Gigliola Clerici for her helpful support with rheological measurements.

REFERENCES

Alfrey Jr., T., Gurnee, E.F., 1956. Dynamics of Viscoelastic Behavior. In: Eirich, F.R. (Ed.), Rheology. Academic Press Inc., New York, pp. 387–429.

Anseth, K.S., Bowman, C.N., Brannon-Peppas, L., 1996. Mechanical properties of hydrogels and their experimental determination. Biomaterials 17, 1647–1657.

Calvet, D., Wong, J.Y., Giasson, S., 2004. Rheological monitoring of polyacrylamide gelation: importance of cross-link density and temperature. Macromolecules 37, 7762–7771.

Chiari, M., Campoleoni, A., Conti, P., Felli, C., Patrosso, M.C., Brogren, C.H., 1996. Electrophoretic separation of biopolymers in a matrix of polyacrylamide covalently linked to agarose. Electrophoresis 17, 473–478.

Chiari, M., D'Alesio, L., Consonni, R., Righetti, P.G., 1995. New types of large-pore polyacrylamide-agarose mixed-bed matrices for DNA electrophoresis: pore size estimation from Ferguson plots of DNA fragments. Electrophoresis 16, 1337–1344.

Dumitriu, R.P., Mitchell, G.R., Vasile, C., 2011. Rheological and thermal behaviour of poly(N-isopropylacrylamide)/alginate smart polymeric networks. Polym. Int. 60, 1398–1407.

Ferry, J.D., 1970. Viscoelastic Properties of Polymers, second ed. John Wiley & Sons, Inc., New York.

Gerstner, A., Csapo, Z., Sasvari-Szekely, M., Guttman, A., 2000. Ultrathin-layer sodium dodecyl sulfate gel electrophoresis of proteins: effects of gel composition and temperature on the separation of sodium dodecyl sulfate-protein complexes. Electrophoresis 21, 834–840.

Görg, A., Weiss, W., Dunn, M.J., 2004. Current two-dimensional electrophoresis technology for proteomics. Proteomics 4, 3665–3685.

Greaser, M., Warren, C., 2012. Protein Electrophoresis in Agarose Gels for Separating High Molecular Weight Proteins. In: Kurien, B.T., Scofield, R.H. (Eds.), Protein Electrophoresis. Humana Press, New York, pp. 111–118.

Manns, J.M., 2011. SDS-polyacrylamide gel electrophoresis (SDS-PAGE) of Proteins. Curr. Protoc. Microbiol. 22, A.3M.1–A.3M.13.

Miller, I., Eberini, I., Gianazza, E., 2010. Other than IPG-DALT: 2-DE variants. Proteomics 10, 586–610.

Oh-Ishi, M., Maeda, T., 2007. Disease proteomics of high-molecular-mass proteins by two-dimensional gel electrophoresis with agarose gels in the first dimension (Agarose 2-DE). J. Chromatogr. B 849, 211–222.

Parthasarathy, M., Debgupta, J., Kakade, B., Ansary, A.A., Islam Khan, M., Pillai, V.K., 2011. Carbon nanotube-modified sodium dodecyl sulfate-polyacrylamide gel electrophoresis for molecular weight determination of proteins. Anal. Biochem. 409, 230–235.

Rabilloud, T., 2002. Two-dimensional gel electrophoresis in proteomics: old, old fashioned, but it still climbs up the mountains. Proteomics 2, 3–10.

Rabilloud, T., Chevallet, M., Luche, S., Lelong, C., 2010. Two-dimensional gel electrophoresis in proteomics: past, present and future. J. Proteomics 73, 2064–2077.

Rabilloud, T., Vaezzadeh, A.R., Potier, N., Lelong, C., Leize-Wagner, E., Chevallet, M., 2009. Power and limitations of electrophoretic separations in proteomics strategies. Mass Spectrom. Rev. 28, 816–843.

Rogowska-Wrzesinska, A., Le Bihan, M.-C., Thaysen-Andersen, M., Roepstorff, P., 2013. 2D gels still have a niche in proteomics. J. Proteomics 88, 4–13.

Roncada, P., Cretich, M., Fortin, R., Agosti, S., De Franceschi, L., Greppi, G.F., Turrini, F., Carta, F., Turri, S., Levi, M., Chiari, M., 2005. Acrylamide–agarose copolymers: improved resolution of high molecular mass proteins in two-dimensional gel electrophoresis. Proteomics 5, 2331–2339.

Suh, M.-H., Ye, P., Datta, A.B., Zhang, M., Fu, J., 2005. An agarose–acrylamide composite native gel system suitable for separating ultra-large protein complexes. Anal. Biochem. 343, 166–175.

Wang, J., Ugaz, V.M., 2006. Using in situ rheology to characterize the microstructure in photopolymerized polyacrylamide gels for DNA electrophoresis. Electrophoresis 27, 3349–3358.